ENCODING WORD ORDER IN COMPLEX EMBEDDINGS

Anonymous authors
Paper under double-blind review

ABSTRACT

Sequential word order is important when processing text. Currently, neural networks (NNs) address this by modeling word position using position embeddings. The problem is that position embeddings capture the position of individual words, but not the ordered relationship (e.g., adjacency or precedence) between individual word positions. We present a novel and principled solution for modeling both the global absolute positions of words and their order relationships. Our solution generalizes word embeddings, previously defined as independent vectors, to continuous word functions over a variable (position). The benefit of continuous functions over variable positions is that word representations shift smoothly with increasing positions. Hence, word representations in different positions can correlate with each other in a continuous function. The general solution of these functions is extended to complex-valued domain due to richer representations. We extend CNN, RNN and Transformer NNs to complex-valued versions to incorporate our complex embedding (we make all code available). Experiments on text classification, machine translation and language modeling show gains over both classical word embeddings and position-enriched word embeddings. To our knowledge, this is the first work in NLP to link imaginary numbers in complex-valued representations to concrete meanings (i.e., word order).

1 INTRODUCTION

Parallelization <-> PE

When processing text, the sequential structure of language is important, but can be computationally costly to model with neural networks (NNs) (Socher et al., 2011) due to the difficulty in parallelization. This has been alleviated by modeling word sequence not on the NN architecture level, but by adding *position embeddings* on the feature level. This has been done by the convolutional sequence model (ConvSeq) (Gehring et al., 2017) and the Transformer model (Vaswani et al., 2017) that replaces recurrent and convolution operations with purely attention mechanisms. More generally, vanilla position embeddings (Gehring et al., 2017) assume that individual word positions are independent and do not consider relations between neighbouring word positions. We posit that *both* the global absolute positions of words *and* their inner sequential and adjacent relationships are crucial in language. This is supported by recent empirical findings by Shaw et al. (2018) and Dai et al. (2019) who show the importance of modeling distance between sequential elements, and explicitly use extra relative position encodings to capture the relative-distance relationship of words.

We present a novel and principled approach to model both the global absolute positions of words and their inner sequential and adjacent relationships as follows: we extend each word embedding, previously defined as an independent vector, as a continuous function over an independent variable i.e., position. The benefit of continuous functions over variable positions is that word representations shift smoothly with increasing positions. Hence, word representations in different positions can correlate with each other in a continuous function. Fig. 1 illustrates this type of word representation with a three-dimensional complex-valued embedding, where the amplitudes $\{r_1, r_2, r_3\}$ denote semantic aspects corresponding to classical word vectors, and periods $\{p_1, p_2, p_3\}$ denote how sensitive the word is to positional information. We further discuss the necessary properties of these functions to model sequential information and obtain a general solution in the form of a complex-valued embedding. Interestingly, there is a direct connection between a specific case of our general embedding and the well-known positional encoding in Vaswani et al. (2017) (see App. A).

We **contribute** (i) a novel paradigm that extends word vectors as continuous functions over changing variables like word position, and (ii) a general word embedding that models word order in

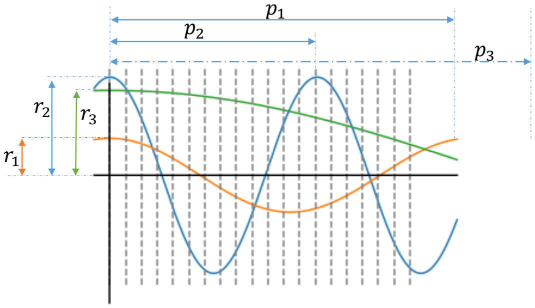

Figure 1: 3-dimensional complex embedding for a single word in different positions. The three wave functions (setting the initial phases as zero) show the real part of the embedding; the imaginary part has a $\frac{\pi}{2}$ phase difference and shows the same curves with its real-valued counterpart. The x-axis denotes the absolute position of a word and the y-axis denotes the value of each element in its word vector. Colours mark different dimensions of the embedding. The three cross points between the functions and each vertical line (corresponding to a specific position pos) represent the embedding for this word in the pos-th position.

a mathematically-sound manner. We integrate our complex word embeddings in state-of-the-art (SOTA) NN architectures (CNN, RNN, Transformer [1]) and experimentally find that it yields gains over both classical word embeddings and position-enriched word embeddings in text classification, machine translation and language modeling. Note that this is the first work in NLP to link imaginary numbers in complex-valued representation to concrete meanings (i.e., word order).

2 Modelling Word Order in Embedding Space

A Word Embedding (WE) generally defines a map $f_{we} : \mathbb{N} \to \mathbb{R}^D$ from a discrete **word** index to a D-dimensional real-valued vector and $\mathbb{N} = \{0, 1, 2, \ldots\}$. Similarly, a Position Embedding (PE) (Gehring et al., 2017; Vaswani et al., 2017) defines another map $f_{pe} : \mathbb{N} \to \mathbb{R}^D$ from a discrete **position** index to a vector. The final embedding for word w_j ($w_j \in \mathbb{W}$ with index j in a given vocabulary $\mathbb{W}$) in the pos-th position in a sentence is usually constructed by the sum

$$f(j, pos) = f_{we}(j) + f_{pe}(pos), \tag{1}$$

and $f(j, pos) \in \mathbb{R}^D$. Since both the word embedding map f_w and the position embedding map f_p only take integer values as word indexes or position indexes, embedding vectors for individual words or positions are trained independently. The independent training for each word vector is reasonable, since a word index is based on the order of a given arbitrary vocabulary and does not capture any specific sequential relationship with its neighboring words. However, the position index captures an ordered relationship, for instance adjacency or precedence, leading to the problem that position embeddings in individual positions (Gehring et al., 2017) are independent of each other; the ordered relationship between positions is not modelled. We refer to this as the *position independence problem.* This problem becomes more crucial when position embeddings are used in position-insensitive NNs, e.g., FastText (Mikolov et al., 2013b), ConvSeq (Gehring et al., 2017) and Transformer (Vaswani et al., 2017), because it is hard for such position-insensitive NNs with vanilla position embeddings (Gehring et al., 2017) to infer that w_{j_1} in the pos-th position is close to w_{j_2} in the $pos + 1$-th position, or that w_{j_1} precedes w_{j_2}; instead, it is only inferred that w_{j_1} and w_{j_2} are in different positions, while the relative distance between them is almost unknown. Thus vanilla position embeddings (Gehring et al., 2017) cannot fully capture the sequential aspect of language.

Next, we first introduce the necessary properties to model word order in embeddings, and then give a unique solution to meet such properties.

$$PE_i \cdot PE_{i+t} = \sum_{j=0}^{\frac{d}{2}-1} \cos c_j t$$

BTW. $PE_i W PE_{i+t} \cancel{\propto} \cos c_j t$

2.1 Extending vectors to functions

In the general definition in Eq. 1, each dimension of the position embedding is obtained based on the discrete position indexes $\{0, 1, 2, ..., \text{pos}, ...\}$. This makes it difficult to model the ordered relationship between the positions. One solution to this problem is to build continuous functions over a variable (i.e., position index) to represent a specific word in an individual dimension. Formally, we define a general embedding as

$$f(j, \text{pos}) = \boldsymbol{g}_j(\text{pos}) \in \mathbb{R}^D, \tag{2}$$

[1] https://github.com/anonymous/anonymous.git

where $\boldsymbol{g}_j$ is short for $\boldsymbol{g}_{we}(j) \in (\mathcal{F})^D$, indicating D functions over position index pos, and $g_{we}(\cdot) : \mathbb{N} \to (\mathcal{F})^D$ is a mapping from a word index to D functions. By expanding the D dimension of $\boldsymbol{g}_j$, a word w_j in the *pos*-th position can be represented as a D-dimensional vector as shown in

$$[g_{j,1}(\text{pos}), g_{j,2}(\text{pos}), ..., g_{j,D}(\text{pos})] \in \mathbb{R}^D, \tag{3}$$

in which $\forall g_{j,d}(\cdot) \in \mathcal{F} : \mathbb{N} \to \mathbb{R}, d \in \{1, 2, ..., D\}$ is a function over the position index pos. To move the word w_j from the current position pos to another one pos', it needs only replace the variable pos to pos' without changing $\boldsymbol{g}_j$.

Functions for words, especially continuous functions, are expected to capture smooth transformation from a position to its adjacent position therefore modeling word order. The *position-independent* position embedding (Gehring et al., 2017) can be considered as a special case of our definition when it only takes independent values for individual positions in the embedding function.

2.2 Properties for the Functions to capture word order

Relative distance is hard to compute because position indices are not visible in NNs after vector embedding (~~discrete position indices are necessarily embedded as vectors like words to be back-propagated with the gradient~~). Hence, we claim that the modeling of relative distance in NNs should be *position-free*: absolute position indices cannot be directly accessed in intermediate layers. Instead of processing *position-free* operations in NNs to capture relative distance between words, prior work (Shaw et al., 2018; Dai et al., 2019) first calculates the relative distance between words, and then feeds the relative distance as an additional feature or as embeddings/weights to NNs, instead of directly feeding with the raw position indices.

Assume that words are embedded into $\mathbb{R}^D$, and let, for $1 \leq d \leq D$, the function $g_{j,d} : \mathbb{N} \to \mathbb{R}$ be the embedding function giving the d-th coordinate of the representation of word w_j (i.e., $g_{j,d}(\text{pos})$ is the d-th coordinate of the embedding of w_j if it occurs at position pos. In the following, we simply write g instead of $g_{j,d}$ when there is no risk of confusion. Ideally, one would like there to exist a function $\text{Transform}_n : \mathbb{R} \to \mathbb{R}$ that transforms the embedding of any word at some position pos to the embedding of a word at position pos $+ n$ such that Transform_n is only dependent on the embedded value itself, but *independent* of the position pos, that is $\forall \text{pos} : g(\text{pos} + n) = \text{Transform}_n(g(\text{pos}))$.

Prior work in NLP (Li et al., 2019), Information Retrieval (Van Rijsbergen, 2004) and Machine Learning (Trabelsi et al., 2017) has shown the usefulness of complex numbers as richer representations. Complex word embeddings (Wang et al., 2019; Li et al., 2019) have been used to model language. To investigate the potential of complex-valued representation, we extend the target domains of $g(\cdot)$ from $\mathbb{R}^D$ to $\mathbb{C}^D$ without losing generality, since real-valued numbers are specific complex numbers with their imaginary part being zero. This property regarding "position-free offset transformation" in complex-valued domains is formally defined in Property 1 below.

unique solution.

Property 1. Position-free offset transformation: An embedding function $g : \mathbb{N} \to \mathbb{C}$ is said to be a *position-free offset transformation* if there exists a function $\text{Transform} : \mathbb{N} \times \mathbb{C} \to \mathbb{C}$ (called the *witness*) such that for all $n \geq 1$, the function $\text{Transform}_n(\cdot) = \text{Transform}(n, \cdot)$ satisfies $\forall \text{pos} \in \mathbb{N} : \boxed{g(\text{pos} + n) = \text{Transform}_n(g(\text{pos}))}$. A position-free offset transformation g is said to be *linearly witnessed* if there is a function $w : \mathbb{N} \to \mathbb{C}$ such that g has a witness Transform satisfying, for all n, $\text{Transform}(n, \text{pos}) = \text{Transform}_n(\text{pos}) = w(n)\text{pos}$ (i.e., each Transform_n is a linear function).

Additionally, a *boundedness* property is necessary to ensure that the position embedding can deal with text of any length (pos could be large in a long document).

Property 2. Boundedness: The function over the variable position should be bounded, i.e. $\exists \delta \in \mathbb{R}^+, \forall \text{pos} \in \mathbb{N}, |g(\text{pos})| \leq \delta$.

Formally, we prove the following claim that there is a unique solution that meets Properties 1 and 2 under the condition that the embedding function is linearly witnessed. We use linear functions because they are well-understood and simple with a single floating-point operation in NNs.

Claim 1. *A function $g : \mathbb{N} \to \mathbb{C}$ is a bounded and linearly witnessed position-free offset transformation iff it is on the form $g(pos) = z_2 z_1^{pos}$ for $z_1, z_2 \in \mathbb{C}$ with $|z_1| \leq 1$.*

Necessity

Proof. Assume that g is a bounded and linearly witnessed position-free offset transformation. Then, by linear witnessing, we have for all pos, $n_1, n_2 \in \mathbb{N}$:

$$\begin{aligned} w(n_1)w(n_2)g(\text{pos}) &= w(n_2)g(\text{pos}+n_1) = g(\text{pos}+n_1+n_2) \\ &= \text{Transform}_{n_1+n_2}(g(\text{pos})) = w(n_1+n_2)g(\text{pos}) \end{aligned}$$

whence $w(n_1+n_2) = w(n_1)w(n_2)$. Write $w(1) = z_1$ and $g(0) = z_2$. As $n_1, n_2 \in \mathbb{N}$ were arbitrary, we have $w(n) = (w(1))^n = z_1^n$ for all $n \in \mathbb{N}$. But then $g(\text{pos}+n) = w(n)g(\text{pos}) = z_1^n g(\text{pos})$. Furthermore, observe that for pos ≥ 1, we have $g(\text{pos}) = g(1+\text{pos}-1) = w(\text{pos})g(0) = z_1^{\text{pos}} z_2 = z_2 z_1^{\text{pos}}$. For pos $= 0$, $g(0) = z_2 = z_2 z_1^0$, whence $\boxed{g(\text{pos}) = z_2 z_1^{\text{pos}},}$ as desired. Observe that if $|z_1| > 1$, then $g(\text{pos})$ is unbounded, whence we have $|z_1| \leq 1$. Conversely, assume that g is on the form $g(\text{pos}) = z_2 z_1^{\text{pos}}$ with $|z_1| \leq 1$. Then, $|g(\text{pos})| \leq |z_2 z_1^{\text{pos}}| \leq |z_2||z_1^{\text{pos}}| \leq |z_2|$, whence g is bounded. Define, for each $n \in \mathbb{N}$, $w(n) = z_1^n$ and $\text{Transform}_n(\text{pos}) = w(n)\text{pos}$. Then, for all pos, $n \in \mathbb{N}$,

Sufficiency

$$g(\text{pos}+n) = z_2 z_1^{\text{pos}+n} = z_2 z_1^{\text{pos}} z_1^n = g(\text{pos}) z_1^n = \text{Transform}_n(g(\text{pos}))$$

showing that g is a linearly witnessed position-free offset transformation. □

For any $z \in \mathbb{C}$, we may write $z = re^{i\theta} = r(\cos\theta + i\sin\theta)$. Thus, for the general form of the embedding g from Theorem 1, we have:

$$g(\text{pos}) = z_2 z_1^{\text{pos}} = r_2 e^{i\theta_2}(r_1 e^{i\theta_1})^{\text{pos}} = r_2 r_1^{\text{pos}} e^{i(\theta_2+\theta_1 \text{pos})} \text{ subject to } |r_1| \leq 1 \tag{4}$$

In implementations, the above definition of g will lead to an optimization problem due to the constraint $|r_1| \leq 1$. A natural and simple way to avoid this is to fix $r_1 = 1$; note that $|e^{ix}| \equiv 1$, thus automatically satisfying the constraint, in contrast to a real-valued embedding where one would need to explicitly devise functions satisfying the constraint. Finally, Eq. 4 can be written in the simplified form: $g(\text{pos}) = re^{i(\omega \text{pos}+\theta)}$. Thus, one can think of g as embedding positions counterclockwise on a complex circle of radius r with a fixed period (r is the amplitude term, θ is the initial phase term, $\frac{\omega}{2\pi}$ is the frequency, and $\frac{2\pi}{\omega}$ is the period term).

2.3 Complex-valued word Embedding

We now define our complex-valued word embedding g as a map taking a word index j and position word index pos to $\mathbb{C}^D$. For a word w_j in position pos, our **general complex-valued embedding** is defined as $f(j, \text{pos}) = \boldsymbol{g}_j(\text{pos}) = \boldsymbol{r}_j e^{i(\boldsymbol{\omega}_j \text{pos}+\boldsymbol{\theta}_j)}$. Therefore, $f(j, \text{pos})$ is defined as:

$$[r_{j,1}e^{i(\omega_{j,1}\text{pos}+\theta_{j,1})}, ..., r_{j,2}e^{i(\omega_{j,2}\text{pos}+\theta_{j,2})}, \cdots, r_{j,D}e^{i(\omega_{j,D}\text{pos}+\theta_{j,D})}] \tag{5}$$

Note that each coordinate d ($1 \leq d \leq D$) has a separate amplitude $r_{j,d}$, period $p_{j,d} = \frac{2\pi}{\omega_{j,d}}$, and initial phase $\theta_{j,d}$. In Fig. 1 each dimension is represented as a wave which is parameterized by an amplitude, a period/frequency, and an initial phase. The trainable parameters of the embedding are the amplitudes vector $\boldsymbol{r}_j = [r_{j,1}, ..., r_{j,D}]$, the period/frequency related weights $\boldsymbol{\omega}_j = [\omega_{j,1}, ..., \omega_{j,D}]$, and the initial phase vector $\boldsymbol{\theta}_j = [\theta_{j,1}, ..., \theta_{j,D}]$. Note that the mean values of $f(j, \cdot)$ over all positions are linearly dependent on the amplitude. Observe that the period/frequency determines to what degree the word is sensitive to the position. With an extremely long period (i.e., ω_j very small), the complex-valued embedding is approximately constant for all possible values of pos, and hence approximates a standard word embedding. Conversely, if the period is short, the embedding will be highly sensitive to the position argument.

In our embedding, the mean vectors of $f(j, \cdot)$ taken over all positions are linearly correlated to the amplitude embedding $\boldsymbol{r}_j = [r_{j,1}, ..., r_{j,K}]$ with a coefficient $\frac{2}{\pi}$. The amplitude $r_{j,d}$ of our embedding depends only on the word w_j (and coordinate d), not on the position of the word, whence one can think of the vector $g_{pe}(j, \text{pos}) = [e^{i(\omega_{j,1}\text{pos}+\theta_{j,1})}, \cdots, e^{i(\omega_{j,D}\text{pos}+\theta_{j,D})}]$ as a "purely" positional embedding. Consequently, our complex embedding can be considered an element-wise multiplication between the word embedding $g_{we}(j) = [r_{j,1}, ..., r_{j,K}]$ and position embedding g_{pe}.

$$f(j, \text{pos}) = g_{we}(j) \odot g_{pe}(j, \text{pos}) \tag{6}$$

Prior work (Gehring et al., 2017; Vaswani et al., 2017) uses mean-weight addition between word embeddings f_{we} and position embeddings f_{pe} (all words share the weights). In our work, word embeddings and position embeddings are decoupled to some extent by element-wise multiplication and

Dataset	train	test	vocab.	task	Classes
CR (Hu & Liu, 2014)	4K	CV	6K	product reviews	2
MPQA (Wiebe et al., 2005)	11k	CV	6K	opinion polarity	2
SUBJ (Pang & Lee, 2005)	10k	CV	21k	subjectivity	2
MR (Pang & Lee, 2005)	11.9k	CV	20k	movie reviews	2
SST (Socher et al., 2013)	67k	2.2k	18k	movie reviews	2
TREC (Li & Roth, 2002)	5.4k	0.5k	10k	Question	6

Table 1: Dataset Statistics. CV means 10-fold cross validation. The last 2 datasets come with train/dev/test splits.

therefore the frequency/period terms (related to $\omega_{j,d}$) can adaptively adjust the importance between semantic and position information for each word and each dimension. In particular, with higher frequency (i.e., large $\omega_{j,d}$), the final embedding will change dramatically with the changing positions, while it can be fixed for any positions with an extremely-small frequency (i.e., small $\omega_{j,d}$). Interestingly, the well-known position embedding in Transformer (Vaswani et al., 2017) can be seen as a degraded version of one of our specific complex word embeddings (see the Appendix A).

3 Experimental Evaluation

We evaluate our embeddings in text classification, machine translation and language modeling.

3.1 Text Classification

Experimental Setup. We use six popular text classification datasets: CR, MPQA, SUBJ, MR, SST, and TREC (see Tab. 1). We use accuracy as evaluation measure based on fixed train/dev/test splits or cross validation, as per prior work. We use Fasttext (Joulin et al., 2016), CNN (Kim, 2014), LSTM and Transformer (Vaswani et al., 2017) as NN baselines[2]. We use each of them: (1) without positional information; (2) with **Vanilla Position Embeddings (PE)** (randomly initialized and updated during training using the sum between word and position vectors (Gehring et al., 2017); (3) with **Trigonometric Position Embeddings (TPE)** (defining position embeddings as trigonometric functions as per Eq. 7); (4) with **Complex-vanilla** word embeddings (where the amplitude embedding is initialized by the pre-trained word vectors, and the phrase embedding is randomly initialized in a range from $-\pi$ to π without considering word order (Wang et al., 2019)); and (5) with our order-aware complex-valued word embeddings, **Complex-order** (which encode position in the phase parts, train the periods, and where the amplitude embedding is also initialized by pretrained word vectors). For more details on the complex-valued extensions of NNs, see App. B and App. C.

Our embedding generally has $3 \times D \times |\mathbb{W}|$ parameters with D-dimensional word vectors and $|\mathbb{W}|$ words, while previous work (Mikolov et al., 2013b; Pennington et al., 2014) usually employs only $D \times |\mathbb{W}|$ parameters for embedding lookup tables. To increase efficiency and facilitate fair comparison with previous work we set initial phases $\boldsymbol{\theta}_j = [\theta_{j,1}, ..., \theta_{j,D}]$ to a shared constant value (such as zero). Furthermore, the period vectors $\omega_{j,d}$ depend on word index j with length $|\mathbb{W}|$ and the coordinate index d with length D. To decrease the number of parameters, one can either use a *word-sharing* scheme (i.e., $\omega_{j,d} = \omega_{\cdot,d}$), or a *dimension-sharing* scheme ($\omega_{j,d} = \omega_{j,\cdot}$), leading to $|\mathbb{W}| * D + |\mathbb{W}|$ and $|\mathbb{W}| * D + D$ parameters in total for the embedding layer.

We search the hyper parameters from a parameter pool, with batch size in $\{32, 64, 128\}$, learning rate in $\{0.001, 0.0001, 0.00001\}$, L2-regularization rate in $\{0, 0.001, 0.0001\}$, and number of hidden layer units in $\{120, 128\}$. We use pre-trained 300-dimensional vectors from word2vec (Mikolov et al., 2013a) in all models except for Transformers. The models with trainable trigonometric position embedding produce nearly identical results compared to the non-trainable version, therefore we report the result of fixed position embeddings as per Vaswani et al. (2017). We adopt narrow convolution and max pooling in CNN, with number of filters in $\{64, 128\}$, and size of filters in $\{3, 4, 5\}$. In all Transformer models, we only use the encoder layer to extract feature information, where the layer is 1, dimension of word and inner hidden are 256 and 512 respectively, and head number is 8.

[2] Graph convolutional networks (GCNs) (Beck et al., 2018; Sahu et al., 2019) also encode positional information. We do not compare against them because they encode positional information inherently as part of the model, which makes redundant any additional encoding of positional information at the embedding level.

Table 2: Text classification accuracy without position embeddings, with random position embeddings (PE), with trigonometric position embeddings (TPE), with complex-valued NNs without position embeddings (complex-vanilla), and with our complex-order embeddings. Superscripts §, †, ‡ and * mean a significant improvement over a baseline without position embeddings §, PE†, TPE‡ and Complex-vanilla * using Wilcoxon's signed-rank test $p<0.05$.

Sentiment

Method	MR	SUBJ	CR	MPQA	SST	TREC
Fasttext	0.765	0.916	0.789	0.874	0.788	0.874
Fasttext-PE	0.774	0.922	0.789	0.882	0.791	0.874
Fasttext-TPE	0.776	0.921	0.796	0.884	0.792	0.88
Fasttext-Complex-vanilla	0.773	0.918	0.79	0.867	0.803	0.872
Fasttext-Complex-order	**0.787**§†‡*	**0.929**§†‡*	**0.800**§†‡*	**0.889**§†‡*	**0.809**§†‡*	**0.892**§†‡*
LSTM	0.775	0.896	0.813	0.887	0.807	0.858
LSTM-PE	0.778	0.915	0.822	0.889	0.811	0.858
LSTM-TPE	0.776	0.912	0.814	0.888	0.813	0.865
LSTM-Complex-vanilla	0.765	0.907	0.810	0.823	0.784	0.784
LSTM-Complex-order	**0.790**§†‡*	**0.926**§†‡*	**0.828**§†‡*	**0.897**§†‡*	**0.819**§†‡*	**0.869**§†‡*
CNN	0.809	0.928	0.830	0.894	0.856	0.898
CNN-PE	0.816	0.938	0.831	0.897	0.856	0.890
CNN-TPE	0.815	0.938	0.836	0.896	0.838	0.918
CNN-Complex-vanilla	0.811	0.937	0.825	0.878	0.823	0.900
CNN-Complex-order	**0.825**§†‡*	**0.951**§†‡*	**0.852**§†‡*	**0.906**§†‡*	**0.864**§†‡*	**0.939**§†‡*
Transformer w/o position embedding	0.669	0.847	0.735	0.716	0.736	0.802
Transformer-PE	0.737	0.859	0.751	0.722	0.753	0.820
Transformer-TPE (Vaswani et al., 2017)	0.731	0.863	0.762	0.723	0.761	0.834
Transformer-Complex-vanilla	0.715	0.848	0.753	0.786	0.742	0.856
Transformer-Complex-order	**0.746**§†‡*	**0.895**§†‡*	**0.806**§†‡*	**0.863**§†‡*	**0.813**§†‡*	**0.896**§†‡*

Table 3: Text classification accuracy. $\star$ means that scores are reported from other papers.

Method	MR	SUBJ	CR	MPQA	SST	TREC
Word2vec Bow (Conneau et al., 2017) $\star$	0.777	0.909	0.798	0.883	0.797	0.836
Sent2Vec (Pagliardini et al., 2017) $\star$	0.763	0.912	0.791	0.872	0.802	0.858
QuickThoughts (Logeswaran & Lee, 2018) $\star$	0.824	0.948	0.860	0.902	-	0.928
InferSent (Conneau et al., 2017) $\star$	0.811	0.924	**0.863**	0.902	0.846	0.882
QPDN (Wang et al., 2019) $\star$	0.801	0.927	0.810	0.870	0.839	0.882

Results. The results are shown in Tab. 2. Our complex-order embeddings outperform all other variations at all times. This gain in effectiveness comes at a negligible (or non-existent) cost in efficiency (it varies per NN architecture – see Fig. 2). CNNs are the best performing NN as expected following Bai et al. (2018). Tranformer NNs benefit the most from our complex-order embeddings, most likely because they are our weakest baseline. To contextualise these results, Tab. 3 shows classification accuracy of five typical approaches on the same datasets (as reported in the original papers). Our complex-order embeddings outperform all methods, except for the CR dataset, where InferSent is marginally better. Overall, our approach is on a par with the SOTA in embeddings.

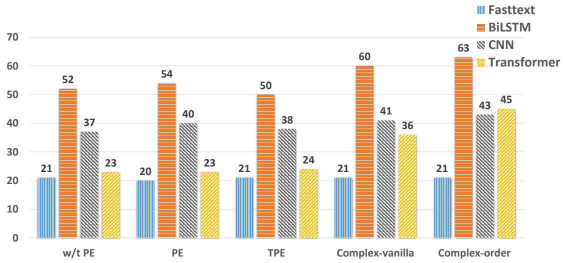

Figure 2: Computation time (seconds) per epoch in Tensorflow on TITAN X GPU.

Table 4: Ablation test for Transformer, showing the effect of (i) the definition of embedding layer($f_d(j, \text{pos})$), and (ii) whether the real-part and imaginary transition share the weights, i.e., $\Re(W^{Q/K/V}) = \Im(W^{Q/K/V})$.

Method	Setting		Params	Accuracy	Δ
	$f_d(j, \text{pos})$	share in $W^{Q/K/V}$			
Transformer-complex-order	$r_{j,d}e^{i(\omega_{j,d}\text{pos})}$	×	8.33M	**0.813**	-
adding initial phases	$r_{j,d}e^{i(\omega_{j,d}\text{pos}+\theta_{j,d})}$	×	11.89M	0.785	-0.028
dimension-sharing period schema	$r_{j,d}e^{i\omega_{j,\cdot}\text{pos}}$	×	5.82M	0.797	-0.016
word-sharing period schema	$r_{j,d}e^{i\omega_{\cdot,d}\text{pos}}$	×	5.81M	0.805	-0.008
dimension-sharing amplitude schema	$r_{j,\cdot}e^{i\omega_{j,\cdot}\text{pos}}$	×	5.82M	0.798	-0.015
word-sharing amplitude schema	$r_{\cdot,d}e^{i\omega_{\cdot,d}\text{pos}}$	×	5.81M	0.804	-0.009
w/t encoding positions (complex-vanilla)	$r_{j,d}e^{i\omega_{j,d}}$	×	9.38M	0.764	-0.049
dimension-sharing period schema	$r_{j,d}e^{i\omega_{j,\cdot}\text{pos}}$	✓	4.77M	0.794	-0.019
word-sharing period schema	$r_{j,d}e^{i\omega_{\cdot,d}\text{pos}}$	✓	4.76M	0.797	-0.016
dimension-sharing amplitude schema	$r_{j,\cdot}e^{i\omega_{j,\cdot}\text{pos}}$	✓	4.77M	0.792	-0.021
word-sharing amplitude schema	$r_{\cdot,d}e^{i\omega_{\cdot,d}\text{pos}}$	✓	4.76M	0.801	-0.012
w/t encoding positions (complex-vanilla)	$r_{j,d}e^{i\omega_{j,d}}$	✓	8.33M	0.743	-0.07
vanilla Transformer (Vaswani et al., 2017)	$WE_{j,d} + PE_d$	-	4.1M	0.761	-0.052

We perform an ablation test (Tab. 4) on Transformer because it is the most common NN to be used with position embeddings. The two period-sharing schemas (dimension-sharing and word-sharing) slightly drop performance, because fewer parameters limit the representative power. Adding initial phases also hurts performance, although we observed that the loss could decrease faster in early epochs compared to the setting without offset. The negative effect of initial phases may be due to periodicity, and $\boldsymbol{\omega}$ cannot be directly regularized with L2-norm penalties. The sharing schemes slightly decrease the performance with less parameters. More details of the learned periods/frequencies (e.g. the distributions of periods/frequencies and case studies) are shown in App. D.

Note that the word-sharing schema outperform the Vanilla Transformer, (both have a comparable number of parameters). If we choose $\Re(W^{Q/K/V}) = \Im(W^{Q/K/V})$, the additional parameters in the embedding layers will affect much less the whole parameter scale in the multiple-layer Transformer, since a embedding layer is only used in the first layer instead of the following Transformer layers.

3.2 Machine Translation

Experimental Setup. We use the standard WMT 2016 English-German dataset (Sennrich et al., 2016), whose training set consists of 29,000 sentence pairs. We use four baselines: basic Attentional encoder-decoder (AED) (Bahdanau et al., 2014); AED with Byte-pair encoding (BPE) subword segmentation for open-vocabulary translation (Sennrich et al., 2016); AED with extra linguistic features (~~morphological, part of speech, and syntactic~~ dependency labels) (Sennrich & Haddow, 2016); and a 6-layer Transformer. Our approach (Transformer Complex-order) uses a batch size of 64, a head of 8, 6 layers, the rate of dropout is 0.1, and the dimension of the word embedding is 512. The embedding layer does not use initial phases, i.e., following $f(j, pos) = \boldsymbol{r}_j e^{i(\boldsymbol{\omega}_j pos)}$. We evaluate MT performance with the Bilingual Evaluation Understudy (BLEU) measure.

Table 5.1: Machine translation results. ⋆marks scores reported from other papers.

Method	BLEU
AED (Bahdanau et al., 2014) ⋆	26.8
AED+Linguistic (Sennrich & Haddow, 2016) ⋆	28.4
AED+BPE (Sennrich et al., 2016) ⋆	34.2
Transformer (Ma et al., 2019) ⋆	34.5
Transformer complex vanilla	34.7
Transformer Complex-order	**35.8**

Table 5.2: Language modeling results. ⋆marks scores reported from other papers.

Method	BPC
BN-LSTM (Cooijmans et al., 2016) ⋆	1.36
LN HM-LSTM (Chung et al., 2016) ⋆	1.29
RHN (Zilly et al., 2017) ⋆	1.27
Large mLSTM (Krause et al., 2016) ⋆	1.27
Transformer XL 6L (Dai et al., 2019)	1.29
Transformer complex vanilla	1.30
Transformer XL Complex-order 6L	**1.26**

Results Tab. 5.1 shows the MT results. Our approach outperforms all baselines. Two things are worth noting: (1) Both the vanilla Transformer and our Transformer Complex-order outperform the three Attentional encoder-decoder baselines which are based on an LSTM encoder and decoder, even when AED uses additional features. (2) Our Transformer Complex-Order outperforms the Vanilla Transformer and complex-vanilla Transformer by 1.3 and 1.1 in absolute BLEU score respectively.

3.3 Language Modeling

Experimental Setup. We use the text8 (Mahoney, 2011) dataset, consisting of English Wikipedia articles. The text is lowercased from a to z, and space. The dataset contains 100M characters (90M for training, 5M for dev, and 5M for testing, as per Mikolov et al. (2012)). We use as baselines BN-LSTM, LN HM-LSTM RHN and Large mLSTM, which are typical recurrent NNs for language modeling in this dataset. We evaluate performance with the Bits Per Character (BPC) measure, (the lower, the better). We run the coder in Dai et al. (2019) with 6 layers for Transformer XL 6L; our model, named Transformer XL complex-order, directly replaces the word embedding with our proposed embedding under the same setting. We choose 6 layers due to limitations in computing resources. For Transformer XL Complex-order, all other parameter settings are as for Transformer XL (Dai et al., 2019). Our complex-order model does not use initial phases.

Results. We see in Tab. 5.2 that our method outperforms all baselines. The first four baselines (BN-LSTM, LN HM-LSTM, RHN and Large mLSTM) are based on recurrent NNs and rely on different regulation methods to become applicable in multiple-layer recurrent architectures. Transformer-based architectures can easily be stacked with multiple layers due to their advantages in parallelization, however the vanilla Transformer does not outperform the multiple-layer recurrent baselines, most likely due to its limitation of 6 layers. Our Transformer XL Complex-order outperforms its vanilla counterpart under the 6-layer setting (and also strong recurrent network baselines), demonstrating that our embedding also generalizes well in tasks with long-term dependency. With limited resources, slightly increasing the parameters in the feature layer like our proposed embedding could be more beneficial than stacking more layers with linearly increasing parameters.

4 Related Work

Complex-valued NNs are not new (Georgiou & Koutsougeras, 1992; Kim & Adalı, 2003; Hirose, 2003). Complex-valued weights have been used in NNs, motivated by biology (Reichert & Serre, 2013), and also as signal processing in speech recognition (Shi et al., 2006). More recently, Arjovsky et al. (2016) shifted RNNs into the complex domain and Wolter & Yao (2018) proposed a novel complex gated recurrent cell. Trabelsi et al. (2017) also developped a complex-valued NN for computer vision and audio processing.

Complex numbers have also been applied to text processing (Van Rijsbergen, 2004; Melucci, 2015). Trouillon et al. (2016) adopt complex embedding for entities in Knowledge Graph Completion to represent antisymmetric relations with Hermitian dot product. Li et al. (2019); Wang et al. (2019) incorporated complex-valued word embeddings with quantum probability driven NNs. However, the physical meaning of both the complex-valued entity and word embeddings is unknown. Further, a complex number has been considered as two real numbers in a black-box learning paradigm (Li et al., 2019; Wang et al., 2019). Our work first links the phase in complex numbers to word position to define concrete physical meaning for complex-valued numbers in document representations.

5 Conclusions

We extended word vectors to word functions with a variable i.e. position, to model the smooth shift among sequential word positions and therefore implicitly capture relative distances between words. These functions are well-defined to model the relative distances, therefore we derive a general solution in complex-valued fashion. Interestingly, the position embedding in Vaswani et al. (2017) can be considered a simplified version of our approach. We extend CNN, RNN and Transformer NNs to complex-valued versions to incorporate our complex embedding. Experiments on text classification, machine translation and language modeling show that our embeddings are more effective than vanilla position embeddings (Vaswani et al., 2017).

REFERENCES

Martin Arjovsky, Amar Shah, and Yoshua Bengio. Unitary evolution recurrent neural networks. In *International Conference on International Conference on Machine Learning*, 2016.

Dzmitry Bahdanau, Kyunghyun Cho, and Yoshua Bengio. Neural machine translation by jointly learning to align and translate. *arXiv preprint arXiv:1409.0473*, 2014.

Shaojie Bai, J. Zico Kolter, and Vladlen Koltun. An empirical evaluation of generic convolutional and recurrent networks for sequence modeling. *CoRR*, abs/1803.01271, 2018. URL `http://arxiv.org/abs/1803.01271`.

Daniel Beck, Gholamreza Haffari, and Trevor Cohn. Graph-to-sequence learning using gated graph neural networks. *arXiv preprint arXiv:1806.09835*, 2018.

Junyoung Chung, Sungjin Ahn, and Yoshua Bengio. Hierarchical multiscale recurrent neural networks. *arXiv preprint arXiv:1609.01704*, 2016.

Alexis Conneau, Douwe Kiela, Holger Schwenk, Loic Barrault, and Antoine Bordes. Supervised learning of universal sentence representations from natural language inference data. *arXiv preprint arXiv:1705.02364*, 2017.

Tim Cooijmans, Nicolas Ballas, César Laurent, Çağlar Gülçehre, and Aaron Courville. Recurrent batch normalization. *arXiv preprint arXiv:1603.09025*, 2016.

Zihang Dai, Zhilin Yang, Yiming Yang, William W Cohen, Jaime Carbonell, Quoc V Le, and Ruslan Salakhutdinov. Transformer-xl: Attentive language models beyond a fixed-length context. *arXiv preprint arXiv:1901.02860*, 2019.

Jacob Devlin, Ming-Wei Chang, Kenton Lee, and Kristina Toutanova. Bert: Pre-training of deep bidirectional transformers for language understanding. *arXiv preprint arXiv:1810.04805*, 2018.

Jonas Gehring, Michael Auli, David Grangier, Denis Yarats, and Yann N Dauphin. Convolutional sequence to sequence learning. In *Proceedings of the 34th International Conference on Machine Learning-Volume 70*, pp. 1243–1252. JMLR. org, 2017.

George M Georgiou and Cris Koutsougeras. Complex domain backpropagation. *IEEE transactions on Circuits and systems II: analog and digital signal processing*, 39(5):330–334, 1992.

Akira Hirose. *Complex-valued neural networks: theories and applications*, volume 5. World Scientific, 2003.

Minqing Hu and Bing Liu. Mining and Summarizing Customer Reviews. pp. 10, 2014.

Armand Joulin, Edouard Grave, Piotr Bojanowski, and Tomas Mikolov. Bag of tricks for efficient text classification. *arXiv preprint arXiv:1607.01759*, 2016.

Taehwan Kim and Tülay Adalı. Approximation by fully complex multilayer perceptrons. *Neural computation*, 15(7):1641–1666, 2003.

Yoon Kim. Convolutional neural networks for sentence classification. *arXiv preprint arXiv:1408.5882*, 2014.

Ben Krause, Liang Lu, Iain Murray, and Steve Renals. Multiplicative lstm for sequence modelling. *arXiv preprint arXiv:1609.07959*, 2016.

Qiuchi Li, Benyou Wang, and Massimo Melucci. Cnm: An interpretable complex-valued network for matching. *arXiv preprint arXiv:1904.05298*, 2019.

Xin Li and Dan Roth. Learning Question Classifiers. In *COLING*. Association for Computational Linguistics, 2002.

Lajanugen Logeswaran and Honglak Lee. An efficient framework for learning sentence representations. *arXiv preprint arXiv:1803.02893*, 2018.

Xindian Ma, Peng Zhang, Shuai Zhang, Nan Duan, Yuexian Hou, Dawei Song, and Ming Zhou. A tensorized transformer for language modeling. *arXiv preprint arXiv:1906.09777*, 2019.

Matt Mahoney. Large text compression benchmark. *URL: http://www. mattmahoney. net/text/text. html*, 2011.

Massimo Melucci. *Introduction to information retrieval and quantum mechanics*, volume 35. Springer, 2015.

T. Mikolov, I. Sutskever, K. Chen, G. Corrado, and J. Dean. Distributed representations ofwords and phrases and their compositionality. *Advances in Neural Information Processing Systems*, 26: 3111–3119, 2013a.

Tomáš Mikolov, Ilya Sutskever, Anoop Deoras, Hai-Son Le, Stefan Kombrink, and Jan Cernocky. Subword language modeling with neural networks. *preprint (http://www. fit. vutbr. cz/imikolov/rnnlm/char. pdf)*, 8, 2012.

Tomas Mikolov, Kai Chen, Greg Corrado, and Jeffrey Dean. Efficient estimation of word representations in vector space. *arXiv preprint arXiv:1301.3781*, 2013b.

Matteo Pagliardini, Prakhar Gupta, and Martin Jaggi. Unsupervised learning of sentence embeddings using compositional n-gram features. *arXiv preprint arXiv:1703.02507*, 2017.

Bo Pang and Lillian Lee. Seeing stars: exploiting class relationships for sentiment categorization with respect to rating scales. pp. 115–124. Association for Computational Linguistics, 2005. doi: 10.3115/1219840.1219855. URL http://portal.acm.org/citation.cfm?doid=1219840.1219855.

Jeffrey Pennington, Richard Socher, and Christopher D Manning. Glove: Global vectors for word representation. In *EMNLP*, volume 14, pp. 1532–1543, 2014.

David P Reichert and Thomas Serre. Neuronal synchrony in complex-valued deep networks. *arXiv preprint arXiv:1312.6115*, 2013.

Sunil Kumar Sahu, Fenia Christopoulou, Makoto Miwa, and Sophia Ananiadou. Inter-sentence relation extraction with document-level graph convolutional neural network. *arXiv preprint arXiv:1906.04684*, 2019.

Rico Sennrich and Barry Haddow. Linguistic input features improve neural machine translation. *arXiv preprint arXiv:1606.02892*, 2016.

Rico Sennrich, Barry Haddow, and Alexandra Birch. Edinburgh neural machine translation systems for wmt 16. *arXiv preprint arXiv:1606.02891*, 2016.

Peter Shaw, Jakob Uszkoreit, and Ashish Vaswani. Self-attention with relative position representations. *arXiv preprint arXiv:1803.02155*, 2018.

Guangji Shi, Maryam Modir Shanechi, and Parham Aarabi. On the importance of phase in human speech recognition. *IEEE transactions on audio, speech, and language processing*, 14(5):1867–1874, 2006.

Richard Socher, Cliff C Lin, Chris Manning, and Andrew Y Ng. Parsing natural scenes and natural language with recursive neural networks. In *Proceedings of the 28th international conference on machine learning (ICML-11)*, pp. 129–136, 2011.

Richard Socher, Alex Perelygin, Jean Wu, Jason Chuang, Christopher D. Manning, Andrew Ng, and Christopher Potts. Recursive Deep Models for Semantic Compositionality Over a Sentiment Treebank. *EMNLP*, pp. 1631–1642, 2013.

Chiheb Trabelsi, Olexa Bilaniuk, Ying Zhang, Dmitriy Serdyuk, Sandeep Subramanian, João Felipe Santos, Soroush Mehri, Negar Rostamzadeh, Yoshua Bengio, and Christopher J Pal. Deep complex networks. *arXiv preprint arXiv:1705.09792*, 2017.

Théo Trouillon, Johannes Welbl, Sebastian Riedel, Éric Gaussier, and Guillaume Bouchard. Complex embeddings for simple link prediction. In *International Conference on Machine Learning*, pp. 2071–2080, 2016.

Cornelis Joost Van Rijsbergen. *The geometry of information retrieval*. Cambridge University Press, 2004.

Ashish Vaswani, Noam Shazeer, Niki Parmar, Jakob Uszkoreit, Llion Jones, Aidan N Gomez, Łukasz Kaiser, and Illia Polosukhin. Attention is all you need. In *Advances in Neural Information Processing Systems*, pp. 5998–6008, 2017.

Benyou Wang, Qiuchi Li, Massimo Melucci, and Dawei Song. Semantic hilbert space for text representation learning. *arXiv preprint arXiv:1902.09802*, 2019.

Janyce Wiebe, Theresa Wilson, and Claire Cardie. Annotating Expressions of Opinions and Emotions in Language. *Language Resources and Evaluation*, 39(2-3):165–210, May 2005. ISSN 1574-020X, 1572-8412. doi: 10.1007/s10579-005-7880-9. URL `http://link.springer.com/10.1007/s10579-005-7880-9`.

Moritz Wolter and Angela Yao. Gated complex recurrent neural networks. *arXiv preprint arXiv:1806.08267*, 2018.

Julian Georg Zilly, Rupesh Kumar Srivastava, Jan Koutník, and Jürgen Schmidhuber. Recurrent highway networks. In *Proceedings of the 34th International Conference on Machine Learning-Volume 70*, pp. 4189–4198. JMLR. org, 2017.

A LINKING TO THE POSITION EMBEDDING IN (VASWANI ET AL., 2017)

Vaswani et al. (2017) proposed a new initialization for position embedding, resulting in comparable performance with previous one (Gehring et al., 2017) even without fine-tuning. The position embedding is empirically selected as

$$\begin{aligned} PE_{2k}(\cdot, pos) &= \sin(pos/10000^{2k/d_{model}}) \\ PE_{2k+1}(\cdot, pos) &= \cos(pos/10000^{2k/d_{model}}) \end{aligned} \tag{7}$$

Where pos is the position index, $2k$ and $2k+1$ is the dimension index and d_{model} is the dimension size of embedding. The reason for choosing this position embedding was not well-explained and its general extension is unknown, leading to some difficulties to improve it.

We claim that the proposed position embedding in (Vaswani et al., 2017) is a degraded version of one of our specific complex word embedding in word-sharing schema (i.e., $\omega_{j,d} = \omega_{\cdot,d}$), in which $p_{j,k} = 2\pi \times 10000^{2k/d_{model}}$ and the initial phases are set as zero. In our complex-valued position embedding, let $f_{pe,k}(\cdot, pos) = e^{i \times 10000^{2k/d_{model}}} = \cos(10000^{2k/d_{model}} pos) + i \sin(10000^{2k/d_{model}} pos)$. Note that there exists a bi-jection between $PE(\cdot, pos)$ and $f_{pe,k}(\cdot, pos)$:

$$\begin{aligned} PE_{2k}(\cdot, pos) &= \Im(f_{pe,k}(\cdot, pos)), \\ PE_{2k+1}(\cdot, pos) &= \Re(f_{pe,k}(\cdot, pos)) \end{aligned} \tag{8}$$

where $\Re$ and $\Im$ are the operations to take the real and imaginary part of a complex-valued number. Its inverse transformation is

$$f_{pe,k}(\cdot, pos) = PE_{2k+1}(\cdot, pos) + iPE_{2k}(\cdot, pos) \tag{9}$$

In our overall embedding, each dimension $f_k(j, pos) = f_{we,k}(j) \odot f_{pe,k}(\cdot, pos)$ in our approaches, while it is $E_k(j, pos) = WE_k(j) + PE_k(\cdot, pos)$ in (Gehring et al., 2017; Vaswani et al., 2017). Hence the position embedding in (Vaswani et al., 2017) is equivalent, albeit not identical, to our complex-valued position embedding with $p_{j,k} = 2\pi \times 10000^{2k/d_{model}}$. It is therefore a particular case of our complex-valued position embedding, the word-sharing schema in which all words share the same period at a certain dimension, i.e, $p_{j,k} = p_{\cdot,k}$ is irrelevant to the choice of j.

B Integrating complex-valued embedding to general neural networks

Neural networks are typically given real numbers as inputs and return real numbers as outputs. To accommodate complex numbers as in- and output, we devise a complex-valued version of various neural network layers i.e. complex-valued FastText with dense layer, CNN, and RNN. Unlike existing complex-valued neural networks (Trabelsi et al., 2017; Wolter & Yao, 2018), our feature layers are also converted into complex-valued layers.

Complex-valued FastText FastTest (Joulin et al., 2016) is a simple and efficient neural network architecture using a dense layer over the sum of all word embeddings for general text classification. For a linear dense layer, i.e., $\boldsymbol{z} = \text{dense}(\boldsymbol{x} + i\boldsymbol{y})$, where $\boldsymbol{x} + i\boldsymbol{y}$ and $\boldsymbol{z}$ denote the complex-valued in- and output, respectively. Let $\boldsymbol{W} = \boldsymbol{A} + i\boldsymbol{B}$ and $\boldsymbol{b} = \boldsymbol{c} + i\boldsymbol{d}$ be complex-valued linear weights and bias, respectively. Then, the complex-valued dense layer is given by:

$$\boldsymbol{z} = \sigma\left(\boldsymbol{Ax} - \boldsymbol{By} + \boldsymbol{c}\right) + i\sigma(\boldsymbol{Bx} + \boldsymbol{Ay} + \boldsymbol{d}) \tag{10}$$

where σ is a real-valued activation function such as the sigmoid function. By rewriting (10) in matrix form (Trabelsi et al., 2017), we obtain:

$$\begin{bmatrix}\Re(z)\\ \Im(z)\end{bmatrix} = \begin{bmatrix}\sigma(\boldsymbol{Ax} - \boldsymbol{By} + \boldsymbol{c})\\ \sigma(\boldsymbol{Bx} + \boldsymbol{Ay} + \boldsymbol{d})\end{bmatrix} \tag{11}$$

where, for $z = x + iy$, $\Re(z) = x$ and $\Im(z) = y$. To save parameters and fairly compare with our real-valued baselines, the weights for real-part and imaginary-part input can be shared, i.e., $\boldsymbol{A} = \boldsymbol{B}, c = d$.

Complex-valued CNN For the complex-valued version of the convolution operation Trabelsi et al. (2017), we similarly define a complex-valued convolution with separate real and imaginary kernels $\boldsymbol{A}$ and $\boldsymbol{B}$, to compute convolutions on the real and imaginary parts of the input in Eq. 10. A complex-valued CNN network is constructed by stacking the operations based on a complex-valued convolution kernel, adding a complex dense layer in (10), and taking their norm as the final prediction in the last layer.

Complex-valued RNN The basic complex RNN formulation is:

$$h_t^C = f\left(\boldsymbol{W}^h \boldsymbol{h}_{t-1} + \boldsymbol{W}^z \boldsymbol{z}_t + \boldsymbol{b}\right) \tag{12}$$

where $\boldsymbol{z}_t$ and $\boldsymbol{h}_t$ represent the complex-valued input and complex-value hidden state vectors at time t, $\boldsymbol{b}$ is a complex-valued bias, $\boldsymbol{W}^h$ and $\boldsymbol{W}^z$ are complex-valued weight transitions for hidden state and input state, and $f\left(\boldsymbol{z}\right) = \sigma\left(\Re\left(\boldsymbol{z}\right)\right) + i\sigma\left(\Im\left(\boldsymbol{z}\right)\right)$ is the activation function. The multiplication $\boldsymbol{W}^h \boldsymbol{h}_{t-1}$ and $\boldsymbol{W}^z \boldsymbol{z}_t$ is computed as defined in (10) above. Similarly, the complex-valued gates are used in LSTM via operations as in (12). In the final layer, a $l2$-norm operation is adopted to obtain a real-valued loss for backpropagation.

Complex-valued Transformer The main components in the Transformer are self-attention sublayers and position-wise feed-forward (FFN) sublayers. A self-attention sublayer employs h attention heads and the concatenation of all heads is used as the output followed by a parameterized linear transformation. For a sequence embedded as complex-valued vector $input = \{\boldsymbol{w}_1, \boldsymbol{w}_2, ..., \boldsymbol{w}_n\}$, the output of each head is computed as a weighted sum of a linear transformation of the input sequence itself, namely

$$output_i = \sum_j a_{i,j} \boldsymbol{w}_j \boldsymbol{W}^V, \tag{13}$$

where $\boldsymbol{w}_j$ is a complex-valued vector and $\boldsymbol{W}^V$ is a complex linear transformation; therefore $output_i$ is also complex. Hence, $output$ is a sequence of complex-valued vectors with the same shape as $input$. The weight coefficient, $a_{i,j}$, which is defined as in real-valued domain, is calculated as the softmax of the product between complex-valued query vectors and key vectors: $a_{i,j} = \text{softmax}\frac{e_{i,j}}{\sum_{i=1}^{n} e_{i,j}}$, and

$$e_{i,j} = \sqrt{\frac{\Re(z)^2 + \Im(z)^2}{n}}, z = \left(\boldsymbol{w}_i \boldsymbol{W}^Q\right)\left(\boldsymbol{w}_j \boldsymbol{W}^K\right)^\dagger, \tag{14}$$

z is a complex number since $\boldsymbol{w}_i$ and $\boldsymbol{w}_j$ are complex-valued vectors and $\boldsymbol{W}^Q, \boldsymbol{W}^K$ are complex-valued transformation. To extend another variant of Transformer called Transformer XL, we keep its original relative position embedding and additionally replace its word embedding with our proposed embedding.

Correspondingly, the FFN sublayer can easily be extended to a complex-valued version by replacing the real-valued layers with complex-valued ones. We use batch-normalization separately for the real and imaginary parts.

C Implementation of the proposed embedding

Words functions are implemented in neural networks by storing the function parameters $\{\boldsymbol{r}, \boldsymbol{\omega}, \boldsymbol{\theta}\}$ and then construct the values based on the arguments. Based on the definition, the implementation of the proposed embedding can easily be implemented with only modifying the embedding layer. We list the basic code to construct our general embedding as below:

```
import torch
import math
class ComplexNN(torch.nn.Module):
    def __init__(self, opt):
        super(ComplexNN, self).__init__()
        self.word_emb = torch.nn.Embedding(opt.n_token, opt.d_model)
        self.frequency_emb = torch.nn.Embedding(opt.n_token, opt.d_model)
        self.initial_phase_emb = torch.nn.Embedding(opt.n_token, opt.d_model)

    def get_embedding(self, x):

        amplitude = self.word_emb(x)
        frequency = self.frequency_emb(x)
        self.initial_phase_emb.weight = torch.nn.Parameter(self.initial_phase_emb.weight
            % (2 * math.pi))

        sent_len=x.size(-1)
        pos_seq = torch.arange(1, sent_len + 1, 1.0,device=amplitude.device)

        pos_seq = pos_seq.unsqueeze(0).unsqueeze(-1)
        pos_seq = pos_seq.repeat([x.size(0),1,amplitude.size(-1)])

        dimension_bais = self.initial_phase_emb (x)

        enc_output_phase = torch.mul(pos_seq,frequency)+ dimension_bais
        enc_output_real = amplitude * torch.cos(enc_output_phase)
        enc_output_image = amplitude * torch.sin(enc_output_phase)
        # return torch.cat([enc_output_real,enc_output_image],-1)
        return enc_output_real,enc_output_image

    def forward(self, x) :
        return self.get_embedding(x)
    ...
```

Note that both the frequency vectors $\boldsymbol{\omega}$ and initial-phase vectors $\boldsymbol{\theta}$ can be shared between words or dimensions, to save parameters. The proposed embedding can be also used in real-valued neural networks if one directly concatenates the real-part numbers and imaginary-part numbers as a double-size real-valued vector; therefore it could easily be extended in any existing networks without any complex-valued components. For instance, it could be a good extension for Transformer based pretrained models like (Devlin et al., 2018) by enriching the feature layer.

D Visualization of frequencies/periods

After training, we obtain the frequency vector $\boldsymbol{\omega}$ for each word. For each word, the mean value of the absolute frequency values, i.e., $\delta_j = \frac{1}{|D|}\sum_{d=1}^{D}|\omega_{j,d}|$ is considered as a metric to test the positional

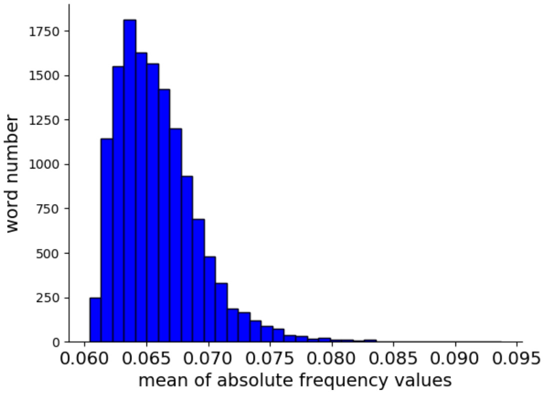

Figure 3: The distribution of the δ_j. Higher values mean that the word representations are more sensitive to the word positions.

sensitivities of the word, since a period value could be negative during training. The density of the δ_j is shown in Fig. 3.

Words with the 50 greatest, and the 50 smallest, frequencies in the SST dataset are shown in Tab. 5. For the words with greatest frequencies, most of them are strong sentiment words like "worst" ,"stupid" and "powerful"; a reason for this may be that such words appear in many positions in many documents during training, and thus they are more sensitive to the positions. Conversely, there are fewer words expressing strong sentiment among words with smaller frequencies, as shown in the second row.

	words
greatest frequencies in descending order	**worst** solid **stupid powerful** mess **wonderful remarkable** suffers intoxicating **thoughtful** **rare** captures portrait gem frontal **terrific unique** wannabe **witty lousy** **pointless** contrived none **worse refreshingly charming** inventive **amazing junk** incoherent refreshing mediocre **unfunny** thinks **enjoyed heartbreaking delightfully** crisp **brilliant** heart spirit **perfectly** nowhere mistake **engrossing fashioned excellent unexpected wonderfully** means
smallest frequencies in ascending order	slowly proposal schemes roiling juliette titles fabric superstar ah wow choreographed **tastelessness** beg **fabulous** muccino jacobi legendary jae rate example code sensation counter deaths hall eun drug mctiernan storylines cellophane wild motion ups trick comedy entertained mission **frightening** witnesses snoots liners african groan satisfaction calm saturday estranged holm refuses **inquisitive**

Table 5: Words with greatest frequencies and frequencies periods (based on δ_j) in SST (a sentiment classification task), all words are converted to lower-case. The strong sentiment words are bold based on manual labeling.